Control of an Autonomous Underwater Vehicle subject to robustness constraints

Juan Luis, Dominique Monnet, Benoit Clement, Fabricio Garelli, Jordan Ninin

Control of an Autonomous Underwater Vehicle subject to robustness constraints ⋆

Juan Luis Rosendo * **Dominique Monnet** ** **Benoit Clement** **
Fabricio Garelli * **Jordan Ninin** **

* *GCA, LEICI, University of La Plata (UNLP), 1900 La Plata, Argentina, (e-mail: juanluisrosendo@gmail.com).*
** *ENSTA Bretagne / Lab-STICC UMR CNRS 6285, 2 rue Francois Verny, F-29200 Brest, France, (e-mail: dominique.monnet@ensta-bretagne.org)*

Abstract: In this paper, we present a method to compute a control law for an Autonomous Underwater Vehicle (AUV) subject to external disturbances. The control law's design objectives are formulated as H_∞ objectives used to synthesize a robust controller. Then, a robustness analysis of AUV model uncertainties is performed without conservatism with interval analysis and global optimization in order to validate the control law. We emphasize the advantage of our approach by comparing it with two other classical design methods with simulations and experiments.

Keywords: Robust control, H_∞ control, AUV, Global optimization, PID design, Robustness Analysis.

1. INTRODUCTION

Applications of underwater robotics are emerging in many different areas. Nowadays, Autonomous Underwater Vehicles (AUV) and Remotely Operated Vehicles (ROV) hold important roles not only for scientific tasks such as seabed mapping and archaeology, but also for defence purposes such as mine hunting. In these different fields tasks like path following, obstacle avoidance and structure inspection are quite common. These kinds of applications, apart from high quality on board sensors, require robust control techniques to deal with the unclear environment where these vehicles operate are required.

The design of control laws for AUV presents three main problems:

- the non-linear dynamics of the vehicle,
- the model uncertainties resulting from the non-exact knowledge of the hydrodynamic coefficients,
- the external disturbance of the environment.

In this work, the approach chosen to deal with these difficulties is the H_∞ approach. There are two main reasons for this: (i) H_∞ synthesis enables to take multiple design constraints into account and (ii) robustness analysis against model uncertainties can be performed with respect to the H_∞ objectives. Several works proposing similar approaches can be found, like (Feng and Allen, 2004) where a synthesizing method for H_∞ controller via singular value truncation is proposed, and (Petrich and Stilwell, 2011) which focuses on the design of a robust multiple-input multiple-output H_∞ controller to deal with a time-varying model. These works suffer from two disadvantages of the traditional H_∞ solving method, the high order of the controller and the lack of robustness with respect to model uncertain parameters. In order to cope with those problems, we propose to use the Matlab's Systune toolbox which enables synthesizing structured controllers from H_∞ specifications and also to perform a robustness procedure to take model uncertainties into account (Apkarian et al., 2015). However, this procedure (Apkarian et al., 2015) cannot ensure, in a guaranteed way, that the design and robustness constraints are reached for all possible values of model uncertain parameters. The sensitivity analysis of design objectives over model uncertainty is a non-convex problem. In order to solve this problem, we propose a global optimization approach which enables performing a robustness analysis in a guaranteed way based on Interval Analysis (see (Kearfott, 1992) and (Monnet et al., 2016)).

This paper is organized as it follows. Section 2 proposes the model of the AUV Ciscrea on which the experiments were conducted, a definition of the H_∞ problem and the robustness analysis. Section 3 addresses the control problem and its implementation. Section 4 presents simulation and experimental results. Finally, in Section 5 proposes a brief discussion of the results.

2. MATERIAL AND METHODS

The aim of this work is to implement a controller robust against both model uncertainties and external disturbances using an approach based on H_∞ synthesis. This section presents the modeling of the robot, a quick introduction to the H_∞ problem, and the robustness analysis.

⋆ This research is supported by DGA (French Defense Procurement Agency), the city of Brest, EIFFEL scholarship from French Government, CONICET (PIP0837) and UNLP(I216), Argentina.

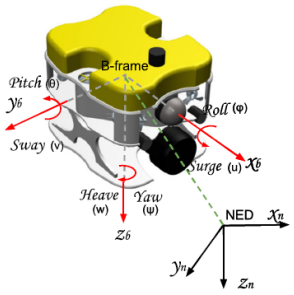

Fig. 1. B-frame and NED-frame of Underwater Vehicles

2.1 Ciscrea Model

The mathematical description of underwater vehicle dynamics is essential for a robust control design. Modeling of underwater vehicles involves two parts of study: kinematics and dynamics. In this work is used the modeling ideas of Fossen (2002) and numerical values obtained in (Yang et al., 2015). Based on Fossen (2002), two coordinate systems are introduced: a NED-frame (North East Down) and a B-frame (Body fixed reference) for the localization as it is described in Fig. 1. In this model, all distances will be in meters, angles in radians and positive clockwise. According to Fossen (2002), rigid-body hydrodynamic forces and moments can be linearly superimposed. Furthermore, the overall non-linear underwater model is characterized by two parts, the rigid-body dynamic (see equation 1) and hydrodynamic formulations included hydrostatics (see equation 2). Parameter definitions are given in Table 1.

$$M_{RB}\dot{\nu} + C_{RB}(\nu)\nu = \tau_{\mathbf{env}} + \tau_{\mathbf{hydro}} + \tau_{\mathbf{pro}} \quad (1)$$

$$\tau_{\mathbf{hydro}} = -M_A\dot{\nu} - C_A(\nu)\nu - D(|\nu|)\nu - \mathbf{g}(\eta) \quad (2)$$

Table 1. Nomenclature of AUV Model

Parameter	Description
M_{RB}	AUV rigid-body mass and inertia matrix
M_A	Added mass matrix
C_{RB}	Rigid-body induced coriolis-centripetal matrix
C_A	Added mass induced coriolis-centripetal matrix
η	Position vector
ν	Velocity vector
$D(\|\nu\|)$	Damping matrix
$\mathbf{g}(\eta)$	Restoring forces and moments vector
$\tau_{\mathbf{env}}$	Environmental disturbances(wind,waves and currents)
$\tau_{\mathbf{hydro}}$	Vector of hydrodynamic forces and moments
$\tau_{\mathbf{pro}}$	Propeller forces and moments vector

In the present application M_{RB} is obtained from Yang et al. (2015). In addition, since the vehicle speed is low C_{RB} and C_A are neglected, then $C(\nu) \approx 0$. The restoring forces and moments vector $\mathbf{g}(\eta)$ are composed of the forces and torque produced by the weight and the buoyancy forces. For Ciscrea robot, buoyancy center and the center of gravity are really close, so it is possible to consider both in the geometrical center of the robot. The marine disturbances, such as wind, waves and current contribute to $\tau_{\mathbf{env}}$. But for an underwater vehicle, only current is considered since wind and waves have negligible effects on AUV during underwater operations. Two hydrodynamic parameters deserve a greater explanation:

- $M_A \in \mathcal{M}_6(\mathbb{R})$: added mass, is a virtual concept representing the hydrodynamic forces and moments. Any accelerating emerged-object would encounter this M_A due to the inertia of the fluid.
- $D(|\nu|) \in \mathcal{M}_6(\mathbb{R})$: damping in the fluid, this parameter consists of four additive parts: Potential damping, wave drift damping, skin friction, and vortex shedding damping. The first two are dismissed in this application, and the others could be approximated by a linear and a quadratic matrices, D_L and D_N respectively, as it is shown in (3) (Yang et al. (2015), Fossen (2002)).

$$D(|\nu|) = D_L + D_N|\nu| \quad (3)$$

In the present work, we focus on the yaw direction to control. Due to the low coupling in the model directions, it is possible to consider that there are no dependencies between the yaw dynamic and dynamics along the other axis. This last observation allows us to get the non-linear model for the yaw dynamic:

$$(I_{YRB} + I_{YA})\ddot{\psi} + (D_{YL} + D_{YN}|\dot{\psi}|)\dot{\psi} = \tau + d, \quad (4)$$

where the parameters are listed in Table 2. Since the yaw speed is mostly between 0 and 4 rad/s to dismiss the coriolis effect in 4 is a reasonable approximation.

Table 2. Model parameters for Yaw dynamic

Parameter	Description
$I_{YRB} = 0.2862$	AUV inertia
$I_{YA} = 0.1104$	Added inertia
$D_{YL} = 0.0945$	Linear damping coefficient
$D_{YN} = 1.4676$	Non-linear damping coefficient
d	Disturbances
τ	Resulting torque produced for all propellers
ψ	Yaw position

To conclude the modeling of the Ciscrea robot, two other assumptions must be addressed: (a) a delay in the compass sensor, which is estimated experimentally at 0.5 seconds. And (b) the non-linear behaviour between the digital command torque T_d and the real torque T_a, in newton, developed by the Ciscrea's thrusters expressed by the following equation:

$$T_a = \begin{cases} 4.7 & if \quad T_d \geq 127 \\ 3.2\max\left(\frac{T_d}{203.874}, \frac{T_d - 30.3781}{65.6756}\right) & if \quad 0 \leq T_d < 127 \\ 4.3\min\left(\frac{T_d}{203.874}, \frac{T_d - 30.3781}{65.6756}\right) & if \quad -127 < T_d < 0 \\ -6.32 & if \quad T_d \leq -127 \end{cases} \quad (5)$$

Further details about this model and its validation can be found in Rosendo et al. (2016).

2.2 H_∞ synthesis

Based on Zhou and Doyle (1998), H_∞ synthesis is an automatic control method to design controllers from frequency specifications. The classical regulation scheme, considered for H_∞ synthesis, is represented in Fig. 2, where K is the controller to compute and P is the plant to control. Both P and K are Linear Time Invariant (LTI) systems. In Fig. 2, w represents the vector of exogenous or perturbation inputs, z the vector of performance outputs, u the control signal and y the measured outputs.
Let $F(P, K)$ be the Linear Fractional Transform of P and

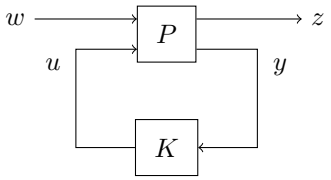

Fig. 2. H_∞ synthesis classical regulation scheme.

K, which maps w into z. $z = F(P,K)w$. We recall that the H_∞ norm of a LTI plant is defined by (6), where σ_{max} is the maximal singular value, $F(P,K)^*$ is the hermitian transpose of $F(P,K)$, ω is the pulsation in rad/s and i the imaginary unit.

$$\|F(P,K)\|_\infty = \sup_{\omega>0} \sigma_{max}\left(F(P,K,i\omega)^* \cdot F(P,K,i\omega)\right) \quad (6)$$

The H_∞ synthesis aims to compute a controller that minimizes the H_∞ norm of $F(P,K)$ and internally stabilizes the closed-loop system. To do so, the following problem is solved:

$$\begin{cases} \min\limits_{K} & \|F(P,K)\|_\infty \\ \text{subject to} & K \text{ stabilizes } F(P,K). \end{cases} \quad (7)$$

From a practical point of view, the H_∞ synthesis computes a controller that minimizes the maximal response of the outputs z to inputs w over the frequencies.
In practice, P is an augmented plant built from G the model of plant to be controlled, and filters that amplify the non-desired behaviors of the objective outputs $\tilde{z}$. z is the weighted counterpart of the outputs $\tilde{z}$, $z = W\tilde{z}$ with W a weighting filter. If both w and z are of dimension one, the H_∞ norm corresponds to the maximum modulus of the transfer from w to z, denoted $T_{w\to z}$, over the pulsations. Then:

$$\begin{aligned} &\|WT_{w\to\tilde{z}}\|_\infty \le 1 \iff \sup_{\omega>0} |W(i\omega)T_{w\to\tilde{z}}(i\omega)| \le 1, \\ &\iff \forall\omega>0,\ |T_{w\to\tilde{z}}(i\omega)| \le |W^{-1}(i\omega)|. \end{aligned} \quad (8)$$

From (8), W^{-1} can be interpreted as a frequency template that bounds the frequency response of $T_{w\to z}$.
The H_∞ synthesis allows taking multiple objectives into account, such as minimization of tracking error, disturbance rejection, etc. Moreover, recent researches have been conducted to synthesize structured controller (Apkarian and Noll (2006), Burke et al. (2006) and Monnet et al. (2016)). Those methods can solve Problem (7) subject to a priori constraints on the controller, for example a PID structure constraint. The last key point is that guaranteed robustness analysis can be performed on the H_∞ norm of a system that suffers from model uncertainties, as it is explained in the following section.

2.3 Robustness analysis

In numerous applications, the model of the system to control suffers from uncertainties. These uncertainties may come from linear approximations or unknown values of physical parameters of the system, for example. They can be taken into account either directly in the synthesis process, or after the synthesis of a controller performed from a nominal model by verifying that this controller ensures the performances for every possible value of the uncertainty. In this section, we focus on the robustness analysis of a controller synthesized for a nominal model with respect to model uncertainty.

Let $G(\sigma)$ be a LTI system which depends on real uncertain parameters $\sigma \in \Sigma$, where Σ denotes the set of admissible value of uncertainties. Suppose that a controller K was synthesized for a nominal plant $G(\sigma_n)$, where $\sigma_n \in \Sigma$ is the central value of uncertainty, from constraints of the kind $\mathcal{C}(G,K) \le 0$. The synthesis constraints $\mathcal{C}$ correspond in our case to stability constraints and H_∞ constraints. Thus, K is a solution to the problem (9).

$$\text{find } K \text{ such that } \mathcal{C}(G(\sigma_n),K) \le 0 \quad (9)$$

The proposed robustness analysis consists in verifying that the constraints are respected for all values of uncertainties:

$$\text{Prove that } \mathcal{C}(G(\sigma),K) \le 0,\ \forall\sigma \in \Sigma \quad (10)$$

The problem (10) is not trivial in the general case, because functions $\mathcal{C}$ are non-convex. Indeed, the stability constraint can be formulated as several polynomial inequalities $R_i(\sigma) \le 0$ using the Routh-Hurwitz criterion (see Jaulin et al. (2001)), and the H_∞ constraints as the modulus of a transfer T, $|T(\sigma,i\omega)| - 1 \le 0$ (see (8)).
In order to solve the problem 10, we propose a global optimization approach based on Interval Analysis (Monnet et al. (2016) and Kearfott (1992)). Interval Analysis combined with branch-and-bound algorithm can provide a guaranteed enclosure $[\underline{\mathcal{C}},\overline{\mathcal{C}}]$ of $sup_{\sigma\in\Sigma}\mathcal{C}$, the maximum of $\mathcal{C}$ over Σ. This corresponds to the worst case among uncertainties:

$$\overline{\mathcal{C}} \le 0 \implies \forall\sigma \in \Sigma,\ \mathcal{C}(G(\sigma),K) \le 0. \quad (11)$$

According to (11), if $\overline{\mathcal{C}} \le 0$, it proves that the constraints are respected for all uncertainties and that K is robust with respect to the model uncertainties. On the opposite, if $\underline{C} > 0$, it proves that there exists at least one value of σ that not satisfies a constraint.
Using our global optimization algorithm to solve Problem (12), it is possible to prove in a guaranteed way whether or not stability constraint and H_∞ constraints are respected for all possible values of σ:

$$\sup_{\sigma\in\Sigma,\omega\in\Omega} \mathcal{C}(G(\sigma,i\omega),K(i\omega)) \quad (12)$$

where Ω is a bounded interval of $\mathbb{R}^+$ (Monnet et al. (2016)).

Remark 1. A global optimization approach to robustness analysis of H_∞ constraints presents an advantage compared to the classical μ-analysis (Young et al., 1991). Indeed, μ-analysis allows computing an upper bound of the frequency response over a finite number of pulsations, whereas global optimization provides an upper bound over all the pulsations in a bounded domain. As a consequence our robustness analysis gives a reliable guarantee that μ-analysis is unable to provide.

3. AUV ROBUST CONTROL IMPLEMENTATION

AUV are usually designed to operate in the ocean environment. This environment is unchecked and the AUV can be subject to external disturbances, such as boat wakes, sea currents, etc. In this section, we propose to synthesize a controller to control the yaw angle of the Ciscrea robot. The control scheme is given by Fig. 3, where r is the reference signal, e the error signal, u the control signal, d the disturbance input and ψ the measure of the yaw angle. The control law must ensure a small tracking error and must not be sensitive to external disturbances. To do

so, H_∞ constraints are defined for a linear model of the yaw behavior of the robot, and the controller is synthesized from these constraints.

The equation that describes the yaw angle dynamics of the

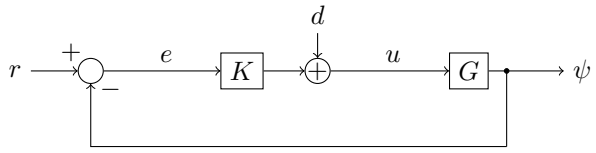

Fig. 3. Control scheme

Ciscrea is given by (4). Since H_∞ synthesis can be applied only on LTI systems, the non-linear system conformed by (4), the non-linear behaviour of actuators and the compass delay are linearized to provide the transfer function:

$$\frac{\psi(s)}{r(s)} = \frac{0.3931}{s^2 + 2.08\delta s} \frac{1 - 0.25s}{1 + 0.25s}. \tag{13}$$

The first rational term corresponds to the yaw dynamics, where δ is the yaw angular velocity at which the system is linearized. Its value can vary between 0 and 4 rad/s. The second rational term corresponds to a first order Pade approximation of the delay. As a consequence, the yaw dynamics is approximated by a family of linear systems resulting from the linearization at different velocities.

The objective is to control the yaw angle with respect to the following criteria:

- The error between the AUV yaw angle and the desired yaw angle must be small.
- The AUV must not be sensitive to torque perturbations due to the environment.
- The control structure is fixed as a filtered Proportional Integral Derivative (PID) controller.

These lead to the synthesis problem (14), where if the norms are under 1, then the specifications are guaranteed.

$$\text{Find } K \text{ such as } \alpha \text{ is minimum} \begin{cases} \|W_e T_{r\to e}\|_\infty \leq \alpha, \\ \|W_e T_{d\to e} W_d\|_\infty \leq \alpha, \\ \|W_u T_{r\to u}\|_\infty \leq \alpha, \\ K \text{stabilizes the closed-loop system.} \end{cases} \tag{14}$$

with

$W_e(s) = \frac{0.1s+0.6283}{s+0.06283}$, $W_d(s) = \frac{0.1s+0.06283}{s+0.6283}$, $W_u = 0.167$.

These criteria can be translated as a small sensitivity of the error signal to the reference and the disturbance input. More precisely, we want the sensitivity to be small in the frequency domain where the robot behaves, that is in the pulsation domain $[0, \omega_c]$, where $\omega_c = 1\ rad/s$ is the cut-off frequency of the closed loop with negative unitary feedback composed of the linear model given by (13). This point leads to the W_e shaping. In addition, we suppose that the spectrum of external disturbances is located in $[0, 0.1]$ Hertz. This point leads to the W_d shaping. In addition, we want to limit the control signal in order to avoid actuator saturation. This point leads to the shaping of W_u.

We propose to synthesize a PID controller with a particular plant $G(\tilde{\delta})$, with $\delta = \tilde{\delta} = 2$. This choice is justified by the trade off between no damping (that leads to very low control command) and (high damping that leads to very high control command). The PID controller has the form: $K(k, s) = k_p + \frac{k_i}{s} + \frac{k_d s}{1+Ts}$ with $k = (k_p, k_i, k_d, T)$. Thus, both transfer functions $T_{r\to e}(k, i\omega)$ and $T_{d\to e}(k, i\omega)$ depend on k. The Matlab's toolbox Systune provides the following solution:

$$\tilde{k} = (4.68, 0.71, 4.68, 0.11).$$

The control law is robust if both stability and H_∞ constraints are respected for all $\delta \in [0, 4]$. This can be proved as true or false in a guaranteed way using interval arithmetic as explained in subsection 2.3. The stability of the closed-loop system can be expressed as a set of four polynomial inequalities with the Routh-Hurwtiz criterion. Using our algorithm based on Interval Analysis, the robustness analysis of the stability constraints provides the following upper bound:

$$\sup_{\delta\in[0,4]} R_i(\delta, \tilde{k}) \leq -0.01, \forall i \in \{1, ..., 4\},$$

which proves that $K(\tilde{k})$ robustly stabilizes the linear closed-loop system. Indeed, the closed-loop system is stable with the controller $\tilde{k}$ for all $\delta \in [0, 4]$.

Moreover, the robustness analysis of H_∞ constraints over the pulsation range $[0, \omega_c]$ provides the following results:

$$\sup_{\delta\in[0,4]} \{\|W_e T_{r\to e}(\tilde{k})\|_\infty\} \in [6.55, 7.20]$$
$$\sup_{\delta\in[0,4]} \{\|W_e T_{d\to e}(\tilde{k}) W_d\|_\infty\} \leq 0.56$$
$$\sup_{\delta\in[0,4]} \{\|W_u T_{r\to u}(\tilde{k})\|_\infty\} \leq 0.89$$

As a consequence, we conclude that one out of three H_∞ constraints is not respected for some values of δ. In order to know for which pulsations and uncertain parameters the frequency template W_e^{-1} is over-passed by the transfer $T_{r\to e}$, the frequency response is plotted in Figure 4 for ten values of the uncertainty δ.

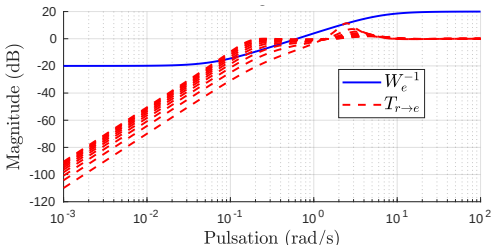

Fig. 4. Bode diagram of $T_{r\to e}$ for diferrent δ values.

It appears in Figure 4 that the closed-loop system does not have the required performance in the pulsation range $[10^{-1.6}, 10^{-0.4}]$ for all values of δ. Over this pulsation range, the gain of the response increases with respect to the value of δ, which means that the frequency template W_e^{-1} is not respected, but only for high angular velocities.

Remark 2. When using H_∞ synthesis, if the H_∞ constraints are not respected the general procedure is to modify the weighting functions to be less demanding with respect to the closed-loop system performances, until a controller is found such that the constraints are respected, i.e. that the performances are guaranteed. In our case, what interests us is to have the best controller with respect to the desired performances. Modifying the weighting functions only to have the H_∞ norm lower than one would degrade the desired controller performances.

Remark 3. In this work we are focusing on the robustness against different operating points. Nevertheless, it would be possible to add in the optimization problem statement (14) extra conditions to match additional robustness features. For example, considering a multiplicative uncertainty.

Even if $K(\tilde{k})$ does not respect one of the H_∞ constraints for some values of δ, the study of the frequency response of the closed-loop system shows that the controller has acceptable performances. In addition, a robust stability analysis enables to guarantee the stability of the linear system, which makes $K(\tilde{k})$ a potentially good controller. Its performance must be validated by simulations with the non-linear model and by experiments. In order to compare the performance of the designed controller, two other PID designs are used. A controller tuned from the Ziegler-Nichols frequency response method, denoted *ZN* controller : $k_{ZN} = (1.32, 0.22, 1.89, 0.5)$, which main design criterion is to obtain a quarter amplitude decay ratio for the load disturbance response. And another controller tune according to the rules exposed in O'Dwyer (2009), denoted the *Chien* controller, for a linear system in the form of (13) and a value of $\delta = 2$: $k_{Chien} = (1.82, 0.12, 6.4, 0.35)$.

4. RESULTS

In this section, the three controllers are compared over simulations and real experiments. The main objective is to show the robustness of the proposed controller (denoted as *Hinf*) against perturbation, and nonlinearities.

4.1 Simulations

The simulations were done using the non-linear model described in the subsection 2.1. Three simulations are presented: a step response, a response to a constant perturbation, and another to a random perturbation. In Fig. 5, a step response of the system can be appreciated. In this figure, the *Hinf* controller has a higher over pass than *Chien* controller, but at the same time the settling time is shorter. This overpass is a consequence of the H_∞ tuning, and actually, this was not considered as a constraint in the design problem.

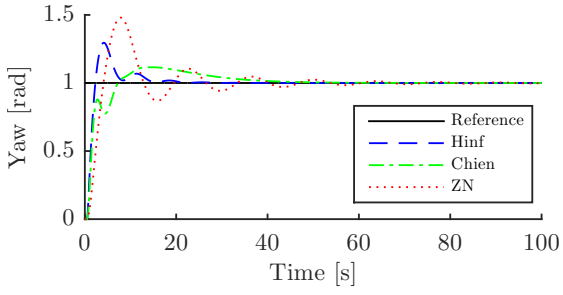

Fig. 5. Step response simulation

Figure 6 shows the response of the system to a step perturbation filtered by W_d, applied to the control input. We can conclude that the *Hinf* controller rejects this perturbation well, contrary to *ZN* and *Chien* controllers which do not take into account perturbation rejection as a constraint in their design process.

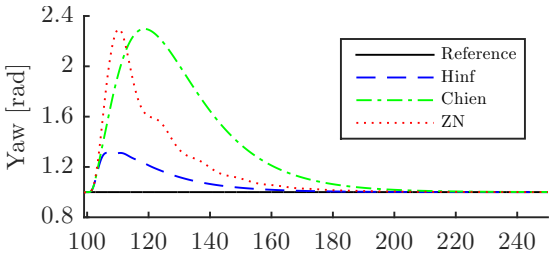

Fig. 6. Constant perturbation simulation

In the last simulation a white uniform noise signal filtered by the weight function W_d (in this way the system is excited in the bandwidth where the disturbances are expected) is applied as a disturbance to the control input. Fig. 7 shows the yaw output. The *Hinf* controller has the best performance in these conditions. Also in Table 3 the Root-Mean-Square Error (RMSE), the Normalized Mean Absolute Error (NMAE) and bias are provided in order to have numerical values to evaluate the performances.

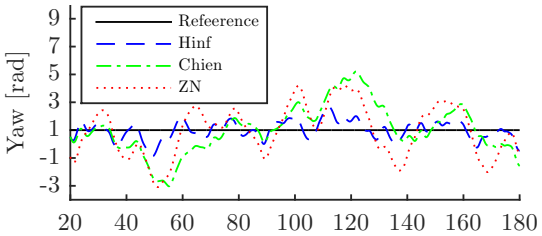

Fig. 7. Step perturbation simulation

Table 3. Random perturbation errors

Simulation	RMSE	NMAE	Bias
ZN	1.7132	2.7969	-0.1263
Hinf	0.6017	1.2138	-0.0480
Chien	1.6816	0.0026	-0.1334

4.2 Experimental Results

The three controllers are compared over three experiments conducted at the ENSTA-Bretagne facilities. Each experiment consists in testing the performance of the three controllers on the real robot subject to perturbations. In all the cases, the perturbation was generated by an external 12V propeller with a constant rotational speed.

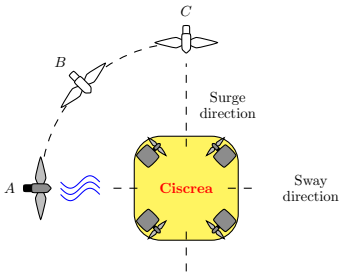

Fig. 8. Top view of experiment setup

The first experiment consists in undergoing the AUV to an external perturbation aligned to its sway direction (see A in Fig. 8). In Figure 9, the yaw measurement is displayed for each controller. In this case between 0 to 40s, the

experimental step response is appreciated, and then at 40s, the external perturbation is applied. From this figure, we can observe the same behaviour as the one predicted by the simulation referred to the step response, and a good rejection of the perturbation for all the techniques employed.

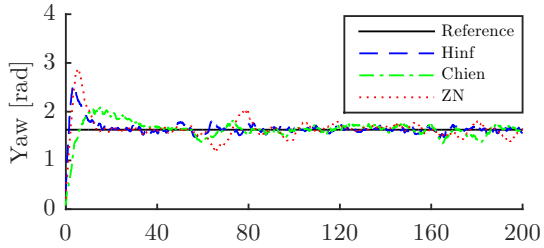

Fig. 9. Perturbation in sway direction

The second experiment consists in exposing the AUV to a perturbation at 45° of sway direction (see B in Fig. 8). In Figure 10, we can see the results and in Table 4, a comparison of the errors between the different controllers. Also in this case the *Hinf* controller shows a better performance and a good rejection of disturbances.

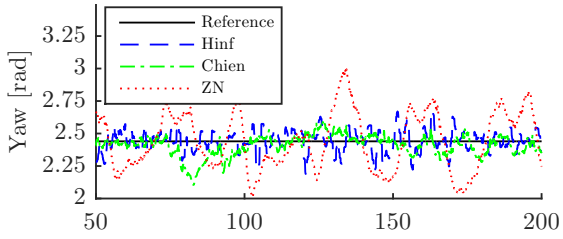

Fig. 10. Perturbation at 45° of surge direction

Table 4. Errors: Perturbation at 45° of surge direction

Experiment	RMSE	NMAE	Bias
ZN	0.1742	0.0502	0.0137
Hinf	0.0650	0.0174	0.0037
Chien	0.0755	0.0179	0.0172

The last experience consists in applying a perturbation in the surge direction (see C in Fig. 8). In Figure 11, the worst perturbation condition is observed. The errors of this experiment are provided in Table 5.

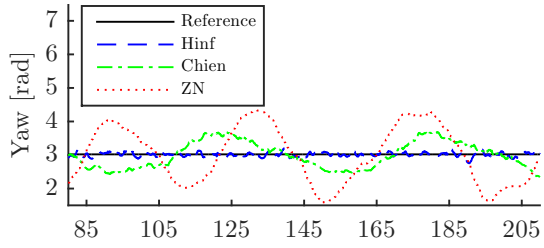

Fig. 11. Perturbation in surge direction

Table 5. Errors: Perturbation in sway direction

Experiment	RMSE	NMAE	Bias
ZN	0.3957	0.0749	-0.0037
Hinf	0.0371	0.0059	-7.1612e-04
Chien	0.2548	0.0482	0.0256

From the three experiments, it appears that the *Hinf* controller has the most robust performance.

5. CONCLUSIONS

This work proposed a methodology fot the analysis and design of a structured control law for a AUV subject to external disturbances. The H_∞ synthesis allows computing a controller which takes three constraints into account at the same time: small tracking error, low sensitivity to external disturbances and saturation avoidance of actuators. A robustness analysis with global optimization tools based on interval analysis enables to analyze which design constraints are reached and to ensure stability over a continuous set of operating angular velocities. The comparison of the controller design from H_∞ constraints with two other controllers obtained from empirical methods, widely used in numerous applications, emphasized the advantages of our approach.

REFERENCES

Apkarian, P. and Noll, D. (2006). Nonsmooth H_∞ synthesis. *Automatic Control, IEEE Transactions on,*, 51(1), 71–86.

Apkarian, P., Dao, M.N., and Noll, D. (2015). Parametric robust structured control design. *IEEE Transactions on automatic Control*, 60(7), 1857–1869.

Burke, J.V., Henrion, D., Lewis, A.S., and Overton, M.L. (2006). Hifoo-a matlab package for fixed-order controller design and H_∞ optimization. *IFAC Proceedings Volumes*, 39(9), 339–344.

Feng, Z. and Allen, R. (2004). Reduced order H_∞ control of an autonomous underwater vehicle. *Control Engineering Practice*, 12(12), 1511–1520.

Fossen, T. (2002). *Marine control systems: Guidance, navigation and control of ships, rigs and underwater vehicles*. Marine Cybernetics Trondheim.

Jaulin, L., Kieffer, M., Didrit, O., and Walter, E. (2001). *Applied Interval Analysis*. Springer London.

Kearfott, R.B. (1992). An interval branch and bound algorithm for bound constrained optimization problems. *Journal of Global Optimization*, 2(3), 259–280.

Monnet, D., Ninin, J., and Clément, B. (2016). A global optimization approach to structured regulation design under H_∞ constraints. *55th IEEE Conference on Decision and Control (CDC), Las Vegas*.

O'Dwyer, A. (2009). *Handbook of PI and PID controller tuning rules*. Imperial College Press.

Petrich, J. and Stilwell, D.J. (2011). Robust control for an autonomous underwater vehicle that suppresses pitch and yaw coupling. *Ocean Engineering*, 38(1), 197–204.

Rosendo, J.L., Clément, B., and Garelli, F. (2016). Sliding mode reference conditioning for path following applied to an auv. *10th IFAC Conference on Control Applications in Marine SystemsCAMS*, 49(23), 8–13.

Yang, R., Clément, B., Mansour, A., Li, M., and Wu, N. (2015). Modeling of a complex-shaped underwater vehicle for robust control scheme. *J Intell Robot Syst*.

Young, P.M., Newlin, M.P., and Doyle, J.C. (1991). Mu analysis with real parametric uncertainty. In *Decision and Control, 1991., Proceedings of the 30th IEEE Conference on*, 1251–1256. IEEE.

Zhou, K. and Doyle, J.C. (1998). *Essentials of Robust Control*. Prentice Hall.